Impurities in a trapped one-dimensional Bose gas of arbitrary interaction strength: Localization-delocalization transition and absence of self-localization

Dennis Breu, Eric Vidal Marcos, Martin Will, and Michael Fleischhauer
Department of Physics and Research Center OPTIMAS, University of Kaiserslautern-Landau, 67663 Kaiserslautern, Germany

(Received 17 October 2024; revised 17 December 2024; accepted 28 January 2025; published 25 February 2025)

We discuss impurities in a one-dimensional Bose gas with arbitrary boson-boson and boson-impurity interactions. To fully account for quantum effects, we employ numerical simulations based on the density-matrix renormalization group (DMRG) and—in the regime of strong boson-boson interactions—the mapping to weakly interacting fermions. A mean-field description of the Bose polaron based on coupled Gross–Pitaevskii Schrödinger equations predicts the existence of a self-localized polaron. We here show that such a solution does not exist and is an artifact of the underlying decoupling approximation. To this end we consider a mobile impurity in a box potential. Our work demonstrates that correlations between the impurity position and the bosons are important even in the limit where mean-field approaches are expected to work well. Furthermore, we derive analytical approximations for the energy of a single polaron formed by a heavy impurity for arbitrary interaction strengths and large but finite boson-boson couplings which accurately reproduce DMRG results. This demonstrates that the polaron problem of a heavy impurity in a one-dimensional Bose gas can be accurately approximated by a proper mean-field description plus a linearized treatment of quantum fluctuations for arbitrary boson-boson and impurity-boson couplings. Finally, we determine the polaron-polaron interaction potential $V(r)$ in the Born-Oppenheimer approximation for small and intermediate distances r, which in the Tonks gas limit is oscillatory due to Friedel oscillations in the Bose gas.

DOI: 10.1103/PhysRevA.111.023326

I. INTRODUCTION

Quasiparticles formed by quantum impurities immersed in a many-body environment play a key role for the understanding of transport phenomena [1]. Furthermore, the interaction of quasiparticles mediated by the host medium forms the basis of many important many-body phenomena in condensed-matter physics [2–5]. In recent years the possibility to experimentally investigate impurities in quantum fluids, such as Bose-Einstein condensates (BEC) of atoms has renewed the interest in these quasiparticles, called Bose polarons. An important difference between Bose polarons in ultracold quantum gases and the Landau-Pekar polaron [6,7] introduced to model electrons interacting with the lattice vibrations of a solid is the large compressibility of the BEC. As a consequence a common theoretical model similar to the Fröhlich model in solids [8], which describes the polaron as interactions of the impurity with phonon excitations, is only suitable for weak boson-boson and weak impurity-boson interactions [9]. In this limit the condensate can be considered undepleted and the role of lattice vibrations is taken over by the Bogoliubov phonons.

For stronger interactions with the impurity the backaction to the condensate needs to be taken into account, while keeping correlations between impurity position and bosons. For translational invariant systems this can be done by means of a Lee-Low-Pines (LLP) transformation [10], which decouples the impurity motion from the many-body problem of interacting bosons. For weak boson-boson interactions g the latter can then be treated rather accurately in a mean-field description for arbitrary strength of the impurity-boson couplings g_{IB} [11–15].

In an inhomogeneous Bose gas and for repulsive impurity-boson interactions, the polaron can localize in density minima of the Bose gas and, similarly to phase separation in multicomponent condensates [16], a localization-delocalization transition can occur. Due to the absence of translational invariance the LLP decoupling does not work here, however. Instead, another mean-field ansatz is often used, which in addition neglects however correlations between impurity position and bosons and results in a coupled Gross–Pitaevskii and Schrödinger equation for the condensate and the impurity, respectively [17–22]. This decoupling mean-field approach (DMF) also predicts a localization transition to occur in translationally invariant systems. In analogy to impurities in liquid ^{4}He [23,24], a single atom can become *self-trapped* in a distortion of the condensate created by the impurity [17–22], thereby spontaneously breaking translational invariance. In two dimensions (2D) and three dimensions (3D) a critical interaction strength is needed for such a self-trapped polaron to exist, but in one dimension (1D) within the DMF approach an arbitrarily small g_{IB} is sufficient [21,22]. Recently it was shown in Ref. [25] that correlations between the center-of-mass motion of the impurity and the bosons suppress this

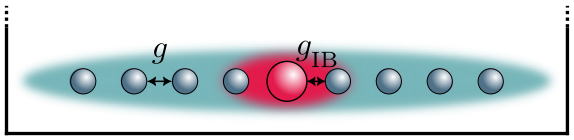

FIG. 1. Mobile quantum impurity in a one-dimensional interacting Bose gas trapped in a box potential. Boson-boson interaction is characterized by coupling strength g and the impurity interacts with the Bose gas with strength g_{IB}.

self-localization transition and solutions with finite localization length only survive for large g_{IB}.

In the present paper we analyze the role of quantum fluctuations to the self-trapping. To this end we consider a mobile impurity of finite mass M in a one-dimensional condensate and employ numerical simulations based on the density-matrix renormalization group (DMRG) [26,27]. Furthermore we consider a box potential, see Fig. 1, to explicitly break translational invariance. For such a system a DMF approach predicts a reentry transition from a *self-localized* polaron at the trap center to a delocalized polaron and eventually to one localized at the potential edge upon changing g_{IB}. We numerically determine the ground-state phase diagram taking quantum fluctuations into account and observe instead only a phase transition between a fully *delocalized* phase for small values of the impurity-boson coupling g_{IB} and a localized phase near one of the edges. Our simulations show that there is no self-trapped solution in the full quantum problem even for very large impurity-boson couplings for which a finite localization length was obtained in Ref. [25].

In Refs. [12–14] we have shown that for a heavy impurity with mass ratios $M/m > O(1)$ in a translational invariant, *weakly interacting* 1D Bose gas, a mean-field approach in an LLP frame gives very accurate predictions for most properties of the polaron, which can further be improved by adding quantum fluctuations perturbatively. We here show that this is also true for a strongly interacting 1D Bose gas. To this end we calculate the polaron energy as a function of g_{IB} for *arbitrary* boson-boson interaction strength ranging from the Bogoliubov regime to the Tonks-gas regime of (nearly) impenetrable bosons. Making use of the mapping between strongly interacting bosons and weakly interacting fermions, we derive an analytical approximation of the polaron energy in the latter regime, which agrees very well with the numerical DMRG data.

Finally we calculate the effective interaction potential between two heavy impurities in the Born-Oppenheimer approximation for short distances. In a weakly interacting Bose gas the potential is monotonic and has a linear slope for small distances [13]. In the limit of (nearly) impenetrable bosons the potential is modified by Friedel-like oscillations, whose long-range behavior has been derived in Refs. [28,29] using a low-energy approximation. We here extend this approach to also capture the short-distance behavior, relevant for bi-polaron bound states.

The paper is organized as follows: In Sec. II we introduce the model. We discuss the problem of self-localization of a finite-mass impurity in a one-dimensional Bose gas in a box potential in Sec. III. Then we discuss a mean-field approach to single polarons formed by a heavy impurity in a strongly interacting Bose gas in Sec. IV. Finally, we derive the short-range interaction potential between two heavy polarons in Born-Oppenheimer approximation in Sec. V.

II. MODEL

The Hamiltonian describing a single quantum impurity in an interacting 1D Bose gas in a box potential of length L has the form ($\hbar = 1$)

$$\hat{H} = \frac{\hat{p}^2}{2M} + \int_{-L/2}^{L/2} \mathrm{d}x \hat{\phi}^\dagger(x) \times \left[-\frac{\partial_x^2}{2m} + \frac{g}{2}\hat{\phi}^\dagger(x)\hat{\phi}(x) + g_{IB}\delta(x-\hat{r}) \right] \hat{\phi}(x), \quad (1)$$

where m (M) is the boson (impurity) mass and g (g_{IB}) the strength of the Bose-Bose (Bose-impurity) s-wave interaction. $\hat{p}$ and $\hat{r}$ represent the momentum and position operators of the impurity in first quantization. $\hat{\phi}(x)$ is the field operator for the bosons. The bosons and the impurity are trapped in an infinitely deep box potential, described by open boundary conditions at $x = \pm L/2$. To quantify the internal interaction strength of the 1D Bose gas we use the unitless Tonks parameter

$$\gamma = \frac{gm}{n_0}, \quad (2)$$

where n_0 is the mean particle density of bosons in the system. The Tonks parameter gives a relation between the interaction ($\propto g n_0^2$) and the kinetic energy ($\propto n_0^3/m$) of the bosons. A large value of γ corresponds to strong boson-boson interactions. For $\gamma \ll 1$ and below a critical temperature a quasicondensate forms. (True condensation is not possible due to the Mermin-Wagner-Hohenberg theorem [30,31].) For $\gamma \to \infty$ the bosons become impenetrable hard-core bosons and can be mapped to free fermions [32].

A powerful method to describe the ground-state of quantum many-body systems in 1D is the density-matrix renormalization group (DMRG) [26]. The DMRG method was originally developed for lattice systems. It can also be applied to continuous models, however, e.g., using a proper discretization, which we apply here. The details of this together with benchmarks are given in the Appendix A.

The Hamiltonian (1) contains both the position and momentum operators $\hat{r}$ and $\hat{p}$ of the impurity, which do not commute. This leads to an entanglement between the motional degrees of freedom of the impurity with the boson field. For translationally invariant systems one can solve this problem by a Lee-Low-Pines (LLP) transformation into a comoving frame [10]. For weak boson-boson interactions and not too small values of the impurity mass the effective Hamiltonian can then be solved rather accurately in a mean-field approximation [12,13], which due to the LLP transformation takes impurity-boson correlations into account.

Without translational invariance, e.g., if the Bose gas (B) and/or the impurity (I) are subject to some trapping potentials $V_{B,I}(x)$ a LLP transformation does not work. Here often another mean-field ansatz is used, which neglects correlations between impurity and bosons and results in a coupled Gross–Pitaevskii and Schrödinger equation for a condensate

wave function $\phi(x)$ and the impurity wave function $\phi_{\rm I}(x)$, respectively:

$$i\partial_t\phi(x,t) = \left(-\frac{\partial_x^2}{2m} + g_{\rm IB}|\phi_{\rm I}(x,t)|^2 + g|\phi(x,t)|^2 + V_B(x)\right)\phi(x,t),$$

$$i\partial_t\phi_{\rm I}(x,t) = \left(-\frac{\partial_x^2}{2M} + g_{\rm IB}|\phi(x,t)|^2 + V_I(x)\right)\phi_{\rm I}(x,t). \quad (3)$$

We show here that, in contrast with a mean-field theory in the LLP frame, this decoupling approach leads to artifacts.

III. LOCALIZATION-DELOCALIZATION TRANSITION IN A BOX POTENTIAL

In Refs. [18,21] it has been argued based on a DMF ansatz, (3), that in a translational invariant homogeneous system the impurity wave function should self-trap in a co-localized distortion of the BEC for small $g_{\rm IB}$. The reality of such self-trapped polarons has been the subject of discussions. Recently it was shown in Ref. [25] that, taking into account leading-order correlations, self trapping only occurs above a certain minimum value of $g_{\rm IB}$.

We now show that, in a full quantum model, self-trapping is absent altogether. To this end we numerically investigate a box potential for bosons and impurity $V_B(x) = V_I(x)$. Here we expect a transition between a delocalized phase, where the impurity is spread out over the whole system, and a localized one, where the impurity is localized at one of the two edges of the system. This is because the energy of an impurity at the edge increases as $E_{\rm loc} \sim \sqrt{g_{\rm IB}}$, while the polaron energy in the bulk scales as $E_p \sim g_{\rm IB}$. Thus for $g_{\rm IB} \to 0$ no edge state exists which only emerges above a critical value of $g_{\rm IB}$. In addition to this a decoupling mean-field theory predicts another phase transition to a self-localized polaron. Due to the broken translational invariance in the box potential considered here, such a self-trapping would manifest itself in a probability density of the impurity centered in the middle of the trap with a width independent of the trap size L.

In the following we investigate both localization phenomena for a weakly interacting as well as a strongly interacting Bose gas using DMRG simulations of the full quantum equations and compare them with numerical solutions and analytical approximations of the DMF equations (3).

A. Localization-delocalization transition in a box potential

We performed DMRG simulations of the ground state of a mobile impurity in a 1D Bose gas in the box potential for different mass ratios M/m and impurity-boson interaction strengths $g_{\rm IB}$. Results for $\gamma = 0.4$ and $\gamma = \infty$ are shown in Figs. 2 and 3, respectively. One recognizes in both cases a sharp transition between a phase where the impurity is delocalized over the trap to a phase where it is localized at one of the two edges. (Note that the true ground state is a superposition of localized states at both edges. Since the energy difference between the symmetric and antisymmetric superpositions vanishes exponentially with increasing system size, the DMRG algorithm converges to a solution on one edge only.) The transition point depends on the boson-boson interaction strength. In the delocalized phase the probability density of the impurity is spread out over the whole system and apart from some corrections at the edges it corresponds to the ground state of the box potential $\approx \cos^2(x\pi/L)$, with L being the length of the box. In the edge-localized phase, on the other hand, the width of the probability distribution becomes independent of system size for large L.

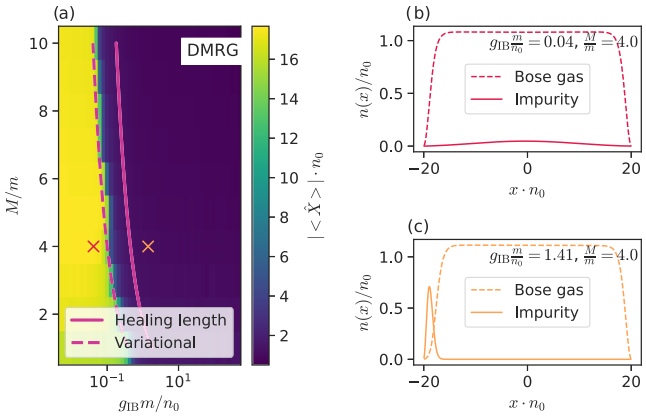

FIG. 2. (a) Localization-delocalization transition of impurity in a box potential in a weakly interacting Bose gas with Tonks parameter $\gamma = 0.4$ and $N = 40$ particles. Color code describes average position $\langle\hat{X}\rangle$ of impurity. The solid line is the prediction from (6) with $l_0 = \xi$. The dashed line gives the prediction with l_0 from a variational ansatz. Panels (b) and (c) show the density distribution corresponding to the two points in panel (a).

A simple estimate for the critical point of the localization-delocalization transition can be obtained as follows: For weak interactions with a Bose gas of density n_0 the energy of a repulsive polaron is given in lowest-order perturbation by

$$E_p \approx g_{\rm IB}n_0, \quad (4)$$

and thus scales linearly in $g_{\rm IB}$.

On the other hand, the energy of an impurity localized at the edge of the condensate can be estimated from the

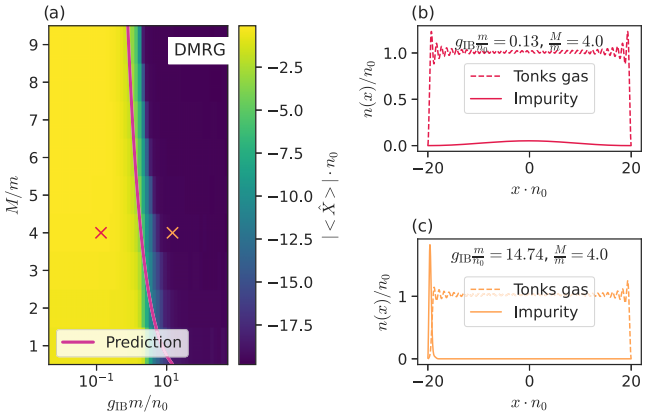

FIG. 3. (a) Localization-delocalization transition of an impurity in a box potential in a Tonks gas ($\gamma = \infty$, $N = 40$). Solid line is prediction from (10). (b), (c) Density distribution corresponding to the two points in panel (a).

repulsive potential created by the bosons, whose density increases quadratically close to the potential edge.

For a weakly interacting Bose gas (small γ) the characteristic length scale $l_0 = \eta\xi$ of the harmonic confinement is the healing length ξ of the Bose condensate. The factor $\eta \simeq O(1)$ accounts for the backaction of the trapped impurity on the density of the condensate near the potential edge, which is relevant in the small-γ regime, due to the large compressibility of the Bose gas. The impurity thus experiences an effective potential for small x:

$$V_{\text{eff}}(x) = \begin{cases} \infty & x \leqslant 0 \\ g_{\text{IB}} n_0 \dfrac{x^2}{2l_0^2} & x > 0. \end{cases}$$

The corresponding oscillator frequency ω follows from $V_{\text{eff}} = \frac{M}{2}\omega^2 x^2$. The ground-state energy of the impurity localized in V_{eff} is thus

$$E_{\text{loc}} \approx \frac{3\omega}{2} = \frac{3}{2}\sqrt{\frac{g_{\text{IB}} n_0}{M l_0^2}}, \tag{5}$$

which scales only with the square root of g_{IB}. Thus for a small impurity-boson interaction no bound state exists. A localized solution emerges only above a critical value

$$\left.\frac{g_{\text{IB}} m}{n_0}\right|_{\text{crit}} = \frac{9}{4\eta^2}\frac{m}{M}\frac{1}{n_0^2\xi^2} = \frac{9}{2\eta^2}\frac{m}{M}\gamma. \tag{6}$$

In Fig. 2(a) we plotted the critical transition line for $\eta = 1$ (solid line). One recognizes that the backaction of the impurity to the condensate needs to be taken into account, which leads to an increased width of the density minimum of the condensate on the left edge, see Fig. 2(c).

One can obtain an approximation for the factor η in (6) from a variational coherent-state ansatz considering a half-infinite system with only one edge at $x = 0$. To this end we assume a factorized ground state $|\psi_{\text{gs}}\rangle = |\phi\rangle|\phi_I\rangle$, with

$$\phi(x) = \sqrt{n_0}\tanh(\alpha x). \tag{7}$$

describing the coherent amplitude of the condensate. $|\phi_I\rangle$ is then the ground state of the impurity in the resulting effective Pöschl-Teller potential, which can be calculated analytically [33]. This approach has already been used to determine bound states of the impurity in a box potential using the ansatz $\alpha = 1/(\sqrt{2}\xi)$ [34]. Here we instead determine the characteristic length scale α by minimizing the total energy. This gives the implicit equation for $\eta = 1/(\sqrt{2}\xi\alpha)$ as a function of the mass ratio M/m, the Tonks parameter γ and $\gamma_{\text{IB}} = g_{\text{IB}} m/n_0$

$$0 = 1 - \eta^2 - \frac{15}{2}\frac{m}{M}\frac{\gamma^{1/2}}{\eta} + \frac{9}{2}\frac{m}{M}\frac{4\gamma_{\text{IB}}\frac{M}{m}\eta^2 + \gamma}{\eta\sqrt{8\gamma_{\text{IB}}\frac{M}{m}\eta^2 + \gamma}}. \tag{8}$$

The solution of this equation is shown in Fig. 2 as a dashed line, showing very good agreement.

In the Tonks gas limit ($\gamma \to \infty$) the hardcore bosons are much less compressible but show Friedel oscillations in the density which also affect the impurity wave function in the localized phase. Hardcore bosons can be mapped to free fermions, which due to Pauli exclusion occupy all single-particle states in the trap up to the Fermi energy. Thus the density of the hardcore gas near one of the edges of the box is given by

$$n(x) \approx \frac{2k_F}{\pi}\left(1 - \frac{\sin(2k_F x)}{2k_F x}\right), \tag{9}$$

with x being the distance from the edge and $k_F = \pi n_0/2$ is the Fermi momentum. The characteristic length scale l_0 is here $(\sqrt{6}/\pi)n_0^{-1}$ which gives the following estimate for the critical g_{IB} of the localization-delocalization transition:

$$\left.\frac{g_{\text{IB}} m}{n_0}\right|_{\text{crit}} = \frac{9}{2}\frac{m}{M}\frac{\pi^2}{6}. \tag{10}$$

In Fig. 3(a) we also plotted this value for comparison and one recognizes reasonable good agreement. Due to the smaller compressibility of the Tonks gas, the localization transition is shifted to higher values of g_{IB}.

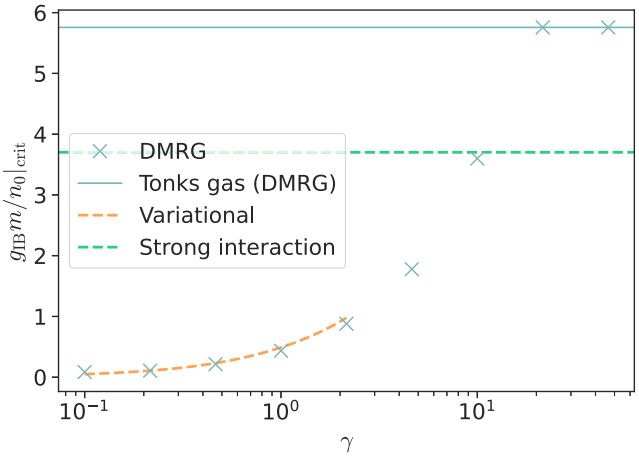

FIG. 4. Critical g_{IB} of the localization-delocalization transition for different Tonks parameters γ, a constant mass ratio $M/m = 2$ and $N = 40$ bosons calculated from DMRG simulations (crosses). Also shown is the critical g_{IB} derived from DMRG simulations of a Tonks gas $\gamma \to \infty$ (solid blue line). These values are compared with the predictions for a weak interacting Bose gas made by the variational ansatz (orange dashed line) and predictions for a Tonks gas (10) (green dashed line).

In Fig. 4 we compare $g_{\text{IB}}|_{\text{crit}}$, obtained from DMRG simulations with the analytic predictions for small, (6), and large Tonks parameters γ, (10). Since the box potential is finite, we determine the transition point of the localization-delocalization transition by calculating at the uncertainty of the impurity position as a function of g_{IB}. At the critical value $g_{\text{IB}}|_{\text{crit}}$ the position uncertainty is maximal. Analytical and numerical values align well up to $\gamma \approx 2.5$, above this value the variational ansatz fails to produce a real value of η. For $\gamma > 10$ the numerical values overshoot the analytic predictions from (10). This is because we approximated the potential produced by the Tonks gas as a harmonic potential.

B. Absence of self-localization in a weakly interacting Bose gas

We now compare the results from DMRG simulations with solutions of the DMF equations (3). In Fig. 5 we show the average position of the impurity as a function of the mass ratio M/m and the impurity-boson interaction g_{IB} from DMRG

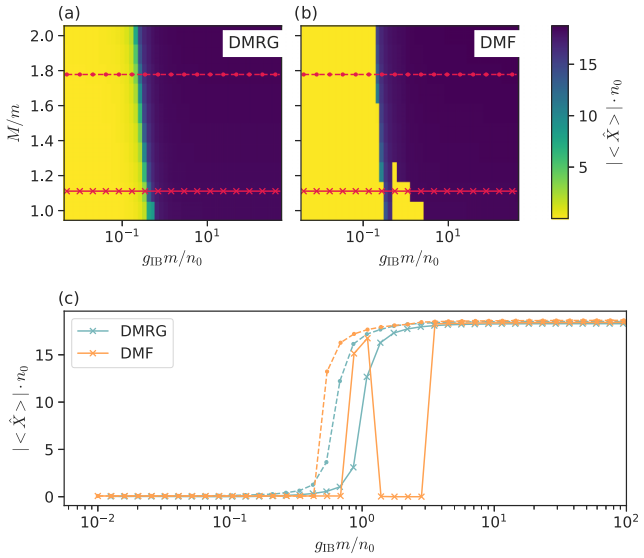

FIG. 5. Comparison between average impurity position $\langle \hat{X} \rangle$ from DMRG and DMF calculations for $\gamma = 0.4$ and $N = 40$. (a) Color plot of $\langle \hat{X} \rangle$ as a function of M/m and g_{IB} obtained by DMRG. Red lines show cuts which are plotted in panel (c). (b) The same obtained from DMF. (c) Cuts in panel (a) for two mass ratios, solid and dashed lines correspond to each other. One clearly recognizes the absence of a self-trapped solution in the DMRG simulations.

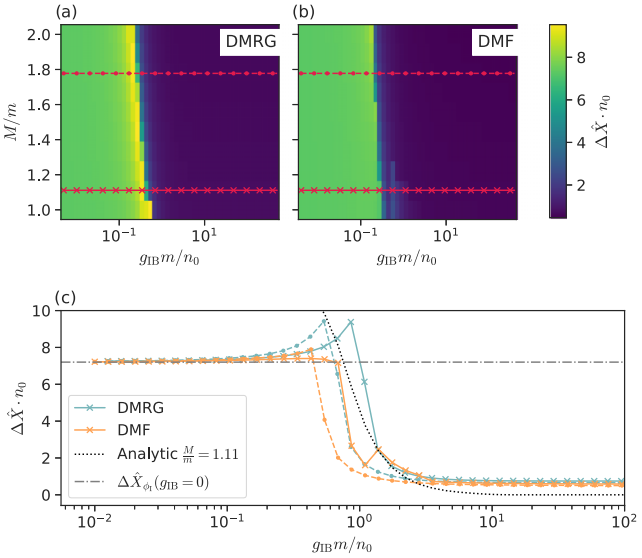

FIG. 6. Comparison between spatial variance of impurity $\langle \Delta\hat{X} \rangle$ from DMRG and DMF for $\gamma = 0.4$ and $N = 40$. (a) Color plot of variance from DMRG simulations as a function of M/m and g_{IB}. Red lines show cuts which are plotted in panel (c). (b) The same obtained from DMF. (c) Cuts in panel (a) for two mass ratios, solid and dashed line correspond to each other. The gray dashed-dotted line shows the spatial width of the impurity expected for $g_{\mathrm{IB}} = 0$. The black dotted line shows the self-localization length λ predicted in DMF for $M/m = 1.11$.

[Fig. 5(a)] and DMF [Fig. 5(b)] simulations for $\gamma = 0.4$, i.e., for weak boson-boson interactions. Figure 5(c) shows a cut for two mass ratios. Since the Tonks parameter is still small, we expect the mean-field simulations to provide good results. And indeed one recognizes that the localization-delocalization transition to the edge of the trap is reasonably well captured by the DMF approach. However, for small mass ratios $M/m < 1.3$ there is an area of coupling strengths around $g_{\mathrm{IB}}m/n_0 \approx 0.5$ where there is a self-localization of the impurity in the middle of the box. Importantly, the width of the impurity distribution in this region is much smaller than the box size, as can be seen in Fig. 6, where we compared the width of the impurity distribution from DMRG and DMF simulations.

In Fig. 7 we plotted the density distributions of bosons and impurity in the box potential for a mass ratio $M/m = 1$ for different values of g_{IB} inside the region of self-trapping predicted by DMF. Also shown is the analytic prediction from Ref. [21] for the impurity probability density in the self-trapping regime,

$$|\phi_{\mathrm{I}}(x)|^2_{\mathrm{TF}} = \frac{1}{2\lambda}\mathrm{sech}^2\left(\frac{x}{\lambda}\right), \tag{11}$$

with $\lambda = (2/\gamma^3)^{1/2}(g/g_{\mathrm{IB}})^2(m/M)n_0^{-1}$ being the localization length, which holds in the Thomas Fermi limit, i.e., for $\lambda \gg n_0^{-1}$.

In summary, the self-localization is an artifact of the decoupling approximation and is not present in the full quantum approach. This is because boson-impurity correlations, which are neglected in DMF, suppress the self-localization [25]. Different from Ref. [25] self-localization does not occur in the full quantum simulations even for large impurity-boson couplings.

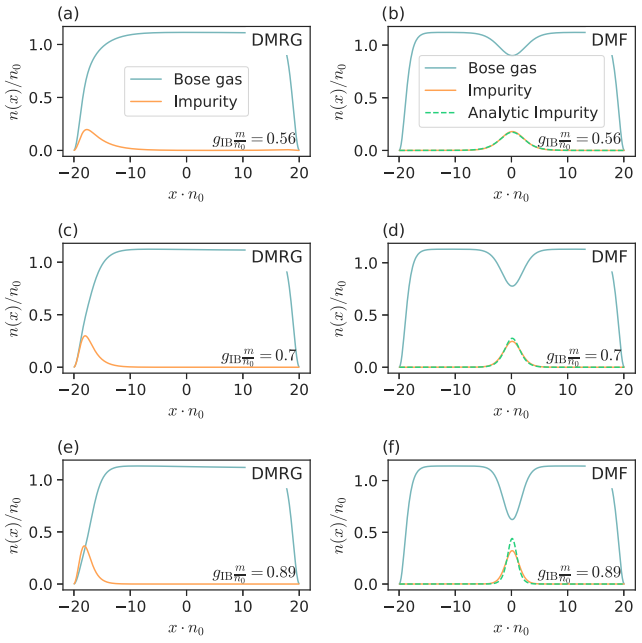

FIG. 7. (left) Density distribution of Bose gas and impurity for different g_{IB} (given in the lower right) from DMRG simulations. (right) The same from mean-field calculations compared with the analytic prediction for a self-trapped polaron, (11). Parameters of the Bose gas are $\gamma = 0.4$, $M/m = 1$, and $N = 40$.

IV. HEAVY POLARON IN A BOSE GAS WITH ARBITRARY BOSON-BOSON INTERACTIONS

In Refs. [12,13] we have shown that key properties of heavy polarons in 1D Bose gases can be rather accurately described by a mean-field theory in an LLP frame that takes into account the backaction of the impurity to the condensate. Quantum fluctuations have to be included only in a linearized approximation. These studies were, however, limited to weak interactions of the bosons, characterized by a Tonks parameter $\gamma < 1$. In the following we show that the opposite case of large Tonks parameters $\gamma \gg 1$ can be accurately treated as well by a perturbation expansion of a complementary mean-field description in the Tonks gas limit.

A characteristic quantity of the polaron is the energy E_P needed to immerse an impurity into the Bose gas $E_P = E(g_{IB} \neq 0) - E(g_{IB} = 0)$. Here $E(g_{IB} = 0)$ is the ground-state energy of the system without Bose-impurity-interaction. In the following we compare analytic and semi-analytic predictions from linearized fluctuation expansions around mean-field approaches in the weak- ($\gamma < 1$) and strong-interaction cases ($\gamma \gg 1$) with exact numerical predictions. To this end we employ DMRG simulations, which agree with previous exact results obtained by Quantum Monte Carlo simulations in Ref. [35].

A. Polaron energy in a weakly interacting Bose gas

For a heavy impurity and a weakly interacting Bose gas, $\gamma \ll 1$, with periodic boundary conditions, a mean-field approximation to the polaron Hamiltonian after a Lee-Low-Pines transformation gives a rather accurate prediction of the polaron energy [11,12,15]:

$$E_P = \frac{4}{3}n\bar{c}\left[1 + \frac{3}{2}\chi + \chi^3 - (1+\chi^2)^{3/2}\right], \tag{12}$$

where the dimensionless parameter $\chi = g_{IB}/(2\sqrt{2}gn\bar{\xi})$ characterizes the impurity-boson interaction strength. If $|\chi| \gtrsim 1$ the condensate undergoes substantial deformation. $\bar{\xi} = \xi\sqrt{m/m_r}$ and $\bar{c} = \sqrt{m/m_r}c$ are the rescaled healing length and speed of sound, respectively. n is the boson density without impurity, and $m_r = (Mm)/(M+m)$ is the reduced mass.

B. Polaron energy in a strongly interacting Bose gas

In the following we discuss the case of a strongly interacting Bose gas, $\gamma \gg 1$. To this end we consider an impurity whose mass is much larger then that of the bosons ($M/m \gg 1$) such that the kinetic energy of the impurity can be neglected. The resulting effective Hamiltonian then reduces to a interacting boson problem in an external δ potential

$$\hat{H} = \int \mathrm{d}x\hat{\phi}^\dagger(x)\left(-\frac{\partial_x^2}{2m} + \frac{g}{2}\hat{\phi}^\dagger(x)\hat{\phi}(x) + g_{IB}\delta(x)\right)\hat{\phi}(x). \tag{13}$$

Figure 8 shows the polaron energy in a strongly ($\gamma = 20$) interacting, trapped 1D Bose gas. The boson density shows Friedel like oscillations, see also Ref. [35], and the characteristic size of the condensate depletion around the fixed position of the impurity is given by the wavelength of these oscillations.

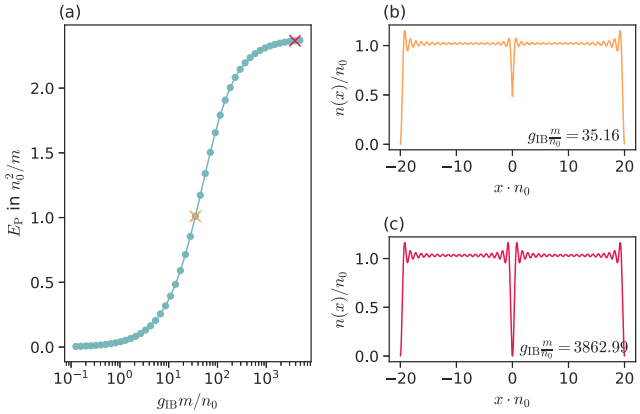

FIG. 8. Polaron in strongly interacting 1D Bose gas with $\gamma = 20$ and $N = 80$ particles in a finite box and $M = \infty$: (a) polaron energy as a function of impurity-boson interaction; (b), (c) wave function for two different values of g_{IB} (written in the lower right) in a box potential and impurity fixed at $x = 0$.

1. *Tonks limit $\gamma \to \infty$*

In the limit $\gamma \to \infty$ the 1D interacting Bose gas maps to free fermions. Here we can calculate the single-particle solutions of free fermions with a infinitely heavy impurity at $x = 0$ for open boundary conditions (OBCs). This system is described by the Hamiltonian

$$\hat{H}_F^0 = \int_{-L/2}^{L/2} \mathrm{d}x\hat{\psi}^\dagger(x)\left(-\frac{\partial_x^2}{2m} + g_{IB}\delta(x)\right)\hat{\psi}(x), \tag{14}$$

with $\{\hat{\Psi}(x), \hat{\Psi}^\dagger(y)\} = \delta(x-y)$. This means we need to solve the problem of noninteracting fermions trapped in a infinitely deep box potential (OBCs) with a delta potential in the middle.

The ground state $|\psi\rangle$ and the ground-state energy E can be written as

$$|\psi\rangle = \int \mathrm{d}x_1 \cdots \int \mathrm{d}x_N \varphi_1(x_1)\cdots\varphi_N(x_N) \times \hat{\psi}^\dagger(x_1)\cdots\hat{\psi}^\dagger(x_N)|0\rangle, \tag{15}$$

$$E = \sum_{l=1}^{N} \frac{k_l^2}{2m}, \tag{16}$$

where the single-particle solutions are given by

$$\varphi_l(x) = a_l \mathrm{sgn}(x)^l \sin\left(k_l\left(|x| - \frac{L}{2}\right)\right). \tag{17}$$

l is an integer and the wave numbers k_l have to be numerically calculated from the boundary condition at the delta potential

$$0 = \frac{k_l}{2m}(1 + (-1)^l) + g_{IB}\tan\left(k_l\frac{L}{2}\right). \tag{18}$$

This then gives for the polaron energy, see Ref. [35],

$$E_p = \frac{n_0^2\pi^2}{2m}\varepsilon(g_{\rm IB}),$$
$$\varepsilon(g_{\rm IB}) = \frac{1}{\pi}\left[\left(1+\frac{\eta^2}{\pi^2}\right)\arctan\frac{\eta}{\pi}+\frac{\eta}{\pi}-\frac{\eta^2}{2\pi}\right], \quad (19)$$

where $\eta = g_{\rm IB}m/n_0 > 0$.

2. *Analytic approximation of the polaron energy for* $1 \ll \gamma < \infty$

For large but finite values of γ one can derive semi-analytic expressions for the polaron energy. As shown by Girardeau [32], bosons with s-wave contact interactions are dual to spin-polarized fermions with p-wave interactions and both can be mapped onto each other by the well-known boson-fermion mapping [32,36]: The bosonic Hamiltonian (13) can be written as a fermionic Hamiltonian

$$\hat{H}_F = \hat{H}_F^0 + \hat{H}_1, \quad (20)$$

with

$$\hat{H}_1 = -\frac{g_{\rm F}}{2}\iint {\rm d}x{\rm d}y\hat{\psi}^\dagger(x)\hat{\psi}^\dagger(y)\frac{\overleftarrow{\partial}}{\partial z}\delta(z)\frac{\overrightarrow{\partial}}{\partial z}\hat{\psi}(y)\hat{\psi}(x), \quad (21)$$

where $z = x - y$ and $\hat{\psi}$ are fermionic field operators. The arrows above the derivatives mean that in the case of the arrow to the left, the derivative has to applied to the function on the left of it and for the arrow to the right on the function to the right. The p-wave interaction strength $g_{\rm F}$ is then related to the bosonic interaction strength g via

$$g_{\rm F} = -\frac{4}{g}. \quad (22)$$

This means a strongly s-wave interacting Bose gas maps to a weakly p-wave interacting Fermi gas and vice versa.

The boson-fermion mapping provides an elegant way to find approximate analytic expressions for the polaron energy in a strongly interacting Bose gas with $\gamma \gg 1$ perturbatively in $|g_{\rm F}| \sim 1/\gamma$.

The second line in (21) can now be treated as perturbation, i.e., $\hat{H}_F = \hat{H}_F^0 + \hat{H}_1$ and the first-order energy correction ΔE_1 reads

$$\Delta E_1 = \langle\psi|\hat{H}_1|\psi\rangle \quad (23)$$
$$= \frac{g_{\rm F}}{2}\sum_{l,n\neq l}^{N}\frac{a_l^2 a_n^2 k_l}{4k_n}[[k_n - k_n\cos(k_nL)]\sin(k_lL) + k_l[k_nL - \sin(k_nL)]]. \quad (24)$$

Figure 9 shows a comparison of the polaron energies as a function of $g_{\rm IB}$ from first-order perturbation in $1/\gamma$, as well as from (12) for small values of γ, with numerical DMRG results. In both cases the polaron energy saturates for increasing $g_{\rm IB}$, which happens when the density of the Bose gas at the position of the impurity approaches zero. One recognizes rather good agreement between analytic approximations and exact simulations both for small and large values of γ even down to $\gamma = 20$ and for all values of $g_{\rm IB}$. Note that the analytic approximation for $\gamma = \infty$ is that from Ref. [35].

Although we have considered here only the case of an impurity with an infinite mass and large values of $\gamma \geqslant 10$ and $\gamma \leqslant 0.1$ one recognizes that key properties of polarons formed by heavy impurities in a 1D Bose gas with arbitrary boson-boson and arbitrary boson-impurity interactions can be obtained rather accurately from a proper mean-field approach and potentially including lowest-order quantum corrections in the Bogoliubov approximation.

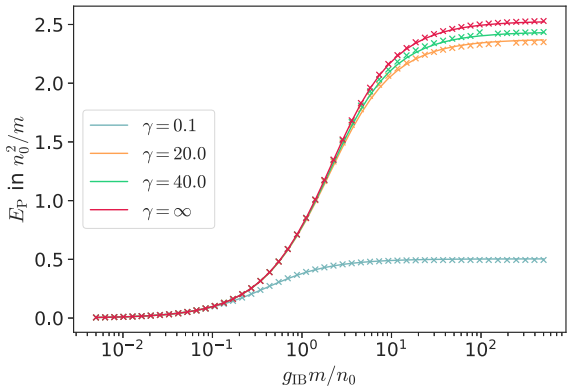

FIG. 9. Comparison of perturbative analytic approximation to polaron energy (solid lines) with DMRG results (crosses) for a strongly interacting 1D Bose gas with $\gamma = 20, 40, \infty$ and $N = 80$ particles, respectively, and $M \to \infty$. In light blue are DMRG results (crosses) compared with mean-field results (solid line) [12,13] for a weakly interacting Bose gas with $\gamma = 0.1$.

V. POLARON INTERACTION IN A STRONGLY INTERACTING BOSE GAS IN THE BORN-OPPENHEIMER LIMIT

Interactions between particles mediated by a many-body environment play an important role in condensed-matter systems. Examples include the Ruderman-Kittel-Kasuya-Yodsia (RKKY) interaction of spins in a Fermi liquid [2–4] and Cooper pairing of electrons [5]. The mechanism responsible for these interactions is the same as what causes the formation of quasiparticles such as the polaron. Even if the impurities do not interact directly with each other, as we assume here, they do so by their coupling to the condensate. If the impurities get close to each other they expel the Bose gas between them and the surrounding gas pushes the impurities together. This causes an effective attractive interaction which in itself can lead to the formation of bound states called bipolaron states. The understanding of bipolarons is one of the key questions of many-body physics. They are suspected to be key for high-temperature superconductivity [37–39] and phenomena such as the electric conductivity of polymers [40–44] or organic magneto-resistance [45].

For a weakly interacting Bose gas ($\gamma \ll 1$) a mean-field ansatz in the LLP frame can be used to obtain semi-analytic expressions of the interaction potential at short distances, which agree very well with quantum Monte Carlo simulations [13]. The mean-field approach does not describe the Casimir-like contributions arising from the exchange of virtual phonons [28,29,46–49], which give, however, only important corrections in the tails of the interaction potential.

In this section we investigate the interaction between Bose polarons in a strongly interacting 1D quasicondensate. In

the Tonks limit $\gamma \to \infty$, where the interacting bosons can be mapped to free fermions, an analytic approximation to the interaction potential has been obtained in Refs. [28,29] using a low-energy Luttinger-liquid approximation

$$V(r) \approx \frac{v_F}{2\pi r}\mathrm{Re}\,\mathrm{Li}_2\left(-\frac{g_{\mathrm{IB}}^2 e^{2\pi i n_0 r}}{(v_F + i g_{\mathrm{IB}})^2}\right), \quad r \gg n^{-1}, \tag{25}$$

with $v_F = \pi n_0/m$ being the Fermi velocity, and Li_2 the dilogarithm function. One notices an oscillatory behavior with the frequency being that of Friedel oscillations. The low-energy approximation gives an accurate description of the large distance behavior of the interaction potential including the Casimir contributions but fails at short distances, which are, however, important for the formation of bipolaron bound states. Thus we here determine the interaction potential both numerically by DMRG simulations and analytically in the Tonks-gas limit for all distances r. Since DMRG is not well suited for periodic boundary conditions, we again assume a confinement of the Bose gas to a box potential. As long as the distance of the impurities from the edges of the box is much larger than the healing length or the Fermi wavelength, boundary effects can be neglected. For the same reason, our simulations, although in principle suitable, do not allow us to accurately extract the far tails of the interaction potential, dominated by virtual phonon exchange. As discussed in the Appendix B, the DMRG simulations reproduce the semi-analytical results from Ref. [13] obtained in mean-field theory for small values of γ.

In the following we calculate the polaron interaction potential in Born-Oppenheimer approximation where $M/m \gg 1$. Here the impurities do not possess kinetic energy and are localized in space. By varying their distance r one can determine the polaron interaction potential $V(r)$ from

$$V(r) = E_{lr}(r) - E_l(r) - E_r(r) + E_0. \tag{26}$$

Here $E_{lr}(r)$ is the ground-state energy with both impurities present, E_l (E_r) the ground-state energy with only the left (right) impurity, and E_0 is the ground-state energy of the Bose gas without any impurities. In the case of two impurities and for $M/m \gg 1$ the Hamiltonian becomes

$$\hat{H}_{\mathrm{B}} = \int \mathrm{d}x \hat{\phi}^\dagger(x)\left(-\frac{\partial_x^2}{2m} + \frac{g}{2}\hat{\phi}^\dagger(x)\hat{\phi}(x)\right)\hat{\phi}(x) + \hat{\phi}^\dagger(x)\left\{g_{\mathrm{IB}}\left[\delta\left(x + \frac{r}{2}\right) + \delta\left(x - \frac{r}{2}\right)\right]\right\}\hat{\phi}(x), \tag{27}$$

where the two impurities are described by the delta potentials at $r/2$ and $-r/2$.

Figure 10 shows the short-distance behavior of $V(r)$ for a medium-sized Tonks parameter $\gamma = 4$ as well as density distributions of the bosons for two different separations r between the impurities. One recognizes a linear potential for small distances similar to the results of Ref. [13] for a weakly interacting Bose gas. The effective potential becomes attractive as soon as the Bose gas between the polarons is substantially diminished. The pressure from the atoms to the left and to the right of the polaron pair then causes a constant force and thus a linear interaction potential.

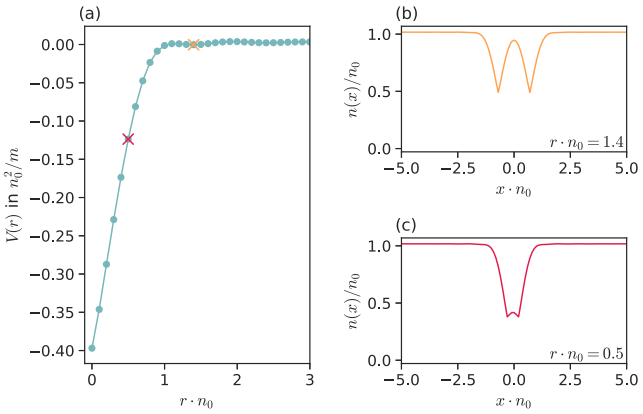

FIG. 10. (left) Interaction potential of heavy impurities in a Bose gas with $\gamma = 4$ and $N = 100$ particles and Bose-impurity interaction strength $g_{\mathrm{IB}}m/n_0 = 1.08$. (right) Density of Bose gas at the two separations indicated in left picture as crosses in the corresponding color.

For large values of γ, on the other hand, oscillations appear in the polaron potential, as can be seen in Fig. 11. The frequency of these oscillations is that of the Friedel oscillations caused by the polarons themselves. As shown in Fig. 11(b), once a single impurity is introduced into the system it causes density oscillation and the second impurity has to displace a smaller or a larger amount of bosons and therefore needs less or more energy to form a polaron. The resulting energy modulations reflect themselves in the polaron potential. Also shown is a comparison to the analytic low-energy approximation (25), which diverges as $r \to 0$.

It can also be seen, that the gradient of the potential increases with the Tonks parameter. This is the case since the force results from the surrounding Bose gas pushing against the polarons. For a stronger interacting Bose gas the resulting

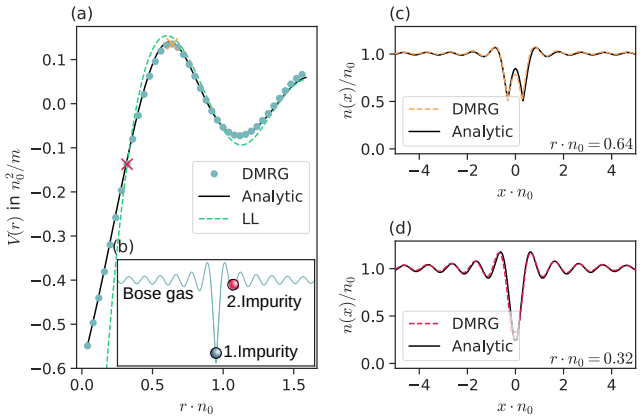

FIG. 11. (Left) Interaction potential of heavy impurities in the Tonks-gas limit $\gamma = \infty$, $N = 80$, and $g_{\mathrm{IB}}m/n_0 = 1.58$. The dashed line shows the Luttinger-liquid approximation from Refs. [28], (25). The inset illustrates the origin of the oscillatory potential. Also shown is the analytic prediction (black line) of the interaction potential obtained from mapping to free fermions in PBC. (right) Density of Bose gas at the two separations indicated in left picture as crosses in the corresponding color.

larger quantum pressure in the gas exerts a bigger force on the polarons.

The interaction potential in the Tonks gas limit can also be obtained directly. To this end we have to calculate the energy of a free Fermi gas (Tonks gas) in a box with periodic boundary conditions in the presence of one or two δ potentials with strength $g_{\rm IB}$ at positions $x = \pm r/2$, which is an elementary quantum mechanics problem. The interaction potential can then be obtained from the total energy $E_{\rm lr}$ of the Tonks gas in the presence of two δ potentials, the energy E_1 of a single δ potential, and the energy without impurities E_0:

$$V(r) = E_{\rm lr} - 2E_1 + E_0. \tag{28}$$

As can be seen in Fig. 11 the bipolaron potential as well as the density distribution of the Tonks gas obtained in this way compare quite well with the DMRG simulations. These results are also in agreement with earlier findings in Ref. [50].

VI. SUMMARY

In the present paper we studied the ground state of a single and two impurities in a one-dimensional Bose gas for arbitrary impurity-boson and boson-boson interactions, addressing: (i) the existence of self-localization of polarons, (ii) the accuracy of mean-field descriptions of polarons which take impurity-boson correlations into account, and (iii) the Born-Oppenheimer interaction potential between two polarons beyond a low-energy approximation. To fully account for quantum effects within the Bose gas, which are particularly important in the limit of large Tonks parameters γ, we performed numerical simulations of a discretized effective lattice model using the density-matrix renormalization group.

In a commonly used mean-field approach to the Bose polaron, condensate and impurity are described by a factorized impurity-boson c-number wave function, leading to a coupled Gross–Pitaevskii Schrödinger equation. Such an approach predicts the existence of a self-trapped polaron for arbitrarily small impurity-boson couplings in a homogeneous 1D gas, where the center of mass of the impurity is localized in a distortion of the condensate created by the impurity. Such a decoupling mean-field (DMF) theory neglects spatial correlations between impurity and bosons. Recent findings have shown that including these correlations in leading order prevents self-trapping for small impurity-boson couplings [25]. We here showed by comparison with exact DMRG results that the self-trapped solution is an artifact of the DMF approach and does not exist also for large impurity-boson interactions.

Mean-field approaches to the Bose polaron in a frame of relative coordinates between bosons and impurity, obtained by a Lie-Low-Pines transformation, amended by a linearized fluctuation analysis, have been shown to provide accurate descriptions of Bose polarons for heavy impurities ($M/m \geqslant 3$) and weak boson-boson interactions ($\gamma \leqslant 1$) [11–13,51,52]. We here showed that the same is true for strongly interacting bosons. To this end we calculated the polaron energy and derived analytical approximations for large but finite Tonks parameters $1 \ll \gamma < \infty$ and arbitrary boson-impurity couplings by using the mapping to weakly interacting fermions.

Finally, we numerically calculated the short-distance interaction potential between two impurities in Born-Oppenheimer approximation for arbitrarily strong boson-boson interactions. For small Tonks parameter $\gamma \leqslant 1$ we verified the results of Ref. [13] were a linear short-distance behavior was predicted. In the strong-interaction limit $\gamma \gg 1$ we found oscillatory modulations in the potential in agreement with low-energy approximations [28,29] and extending them to short distances, relevant for bipolaron bound states.

Note added. Recently, a work by Gomez-Lozada *et al.* appeared studying polarons in 1D lattices of interacting bosons [53], also showing (among other things) that correlations prevent phase separation and self-trapping.

ACKNOWLEDGMENTS

The authors gratefully acknowledge financial support by the DFG through SFB/TR 185, Project No.277625399. E.V.M. furthermore acknowledges support by Fundació Agustí Pedro Pons.

APPENDIX A: DMRG SIMULATION OF QUANTUM IMPURITY IN A 1D BOSE GAS

To apply DMRG for the continuum model let us first look at the Hamiltonian where both bosons and the impurity are described in second quantization:

$$\hat{H} = \int \mathrm{d}x \hat{\phi}^\dagger(x)\left[-\frac{\partial_x^2}{2m} + \frac{g}{2}\hat{\phi}^\dagger(x)\hat{\phi}(x)\right]\hat{\phi}(x) + \int \mathrm{d}x \hat{\phi}_{\rm I}^\dagger(x)\left[-\frac{\partial_x^2}{2M} + g_{\rm IB}\hat{\phi}^\dagger(x)\hat{\phi}(x)\right]\hat{\phi}_{\rm I}(x), \tag{A1}$$

where $\hat{\phi}_{\rm I}$ is the impurity field operator.

Discretization of the x coordinate into a 1D lattice with lattice spacing Δx, the field operators can be replaced by creation and annihilation operators at position $x_i = i\Delta x$,

$$\hat{\phi}(x_i) \to \frac{1}{\sqrt{\Delta x}}\hat{a}_i, \quad \hat{\phi}_{\rm I}(x_i) \to \frac{1}{\sqrt{\Delta x}}\hat{b}_i. \tag{A2}$$

The second-order derivative in (A1) can then be written as

$$\frac{\partial^2}{\partial x^2}\hat{\phi}(x) \approx \frac{\hat{a}_{i-1} - 2\hat{a}_i + \hat{a}_{i+1}}{\Delta x}, \tag{A3}$$

and we set the hoppings which go from and to site 0 and $L+1$ to 0. This is justified because our average system sizes exceed 400 lattice sites were the energy contributions from these hopping terms are small compared with the overall energy. By inserting these transformations into (A1) one arrives at a tight-binding lattice Hamiltonian

$$\hat{H} = \sum_i -J(\hat{a}_i^\dagger\hat{a}_{i+1} + \text{H.c.}) + 2J\hat{a}_i^\dagger\hat{a}_i + \frac{U}{2}\hat{a}_i^\dagger\hat{a}_i^\dagger\hat{a}_i\hat{a}_i - J_{\rm I}(\hat{b}_i^\dagger\hat{b}_{i+1} + \text{H.c.}) + 2J_{\rm I}\hat{b}_i^\dagger\hat{b}_i + U_{\rm I}\hat{b}_i^\dagger\hat{a}_i^\dagger\hat{a}_i\hat{b}_i, \tag{A4}$$

where

$$J = \frac{1}{2m\Delta x^2}, \quad U = \frac{g}{\Delta x}, \tag{A5}$$

$$J_{\rm I} = \frac{1}{2M\Delta x^2}, \quad U_{\rm I} = \frac{g_{IB}}{\Delta x}. \tag{A6}$$

Here the terms containing $\hat{a}_i^\dagger\hat{a}_{i+1}$ ($\hat{b}_i^\dagger\hat{b}_{i+1}$) describe the hopping between lattice sites for the bosons (impurity) with

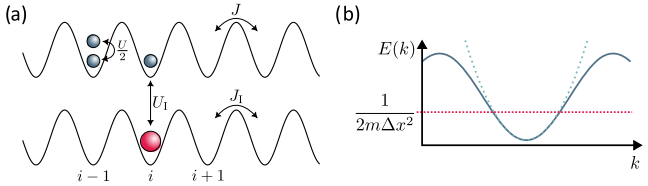

FIG. 12. (a) Illustration of terms in Hamiltonian (A4). The blue circles depict bosons which interact with strength $U/2$ and can hop with amplitude J. The impurity is shown as a red circle. It interacts with the bosons with strength U_I and hops between lattice sites with amplitude J_I. (b) Comparison between the sinusoidal dispersion relation of particles in a lattice to that of free particles, with the maximal energy to which both remain comparable.

hopping amplitude J (J_I). The diagonal terms $\approx \hat{a}_i^\dagger \hat{a}_i$ (or $\hat{b}_i^\dagger \hat{b}_i$) describe a local potential at site i for the bosons (impurity). The strength of this potential is also given by the hopping amplitude J (J_I). It does not effect the dynamics of the system but needs to be taken into account when calculating the ground-state energy. The terms proportional to $\hat{a}_i^\dagger \hat{a}_i^\dagger \hat{a}_i \hat{a}_i$ ($\hat{b}_i^\dagger \hat{a}_i^\dagger \hat{a}_i \hat{b}_i$) relate to the interaction between the bosons (bosons and impurity). The strength of this interaction is given by U (U_I). A graphical illustration of the terms of Hamiltonian (A4) is given in Fig. 12(a).

The discrete Hamiltonian is only a faithful approximation to the continuous model in the low-energy regime. Particles in a lattice possess a sinusoidal dispersion relation while free particles have a parabolic one [see Fig. 12(b)]. The two dispersion relations agree for up to a maximum energy of $1/2m\Delta x^2$ which relates to the hopping amplitude of the bosons J in the discrete system. So the energy per lattice site caused by the interaction between the bosons needs to be lower then the hopping amplitude J. This leads to the condition

$$\tilde{n}_0 U \ll J, \tag{A7}$$

where $\tilde{n}_0$ is the mean particle number per lattice site. In terms of the unitless Tonks parameter γ this can be expressed as

$$\gamma \tilde{n}_0^2 \ll 1. \tag{A8}$$

Thus, for larger Tonks parameter γ, the mean particle number $\tilde{n}_0$ per lattice site needs to be kept low enough such that the discrete system remains a faithful approximation to the continues one.

In addition to the fact that the discrete system needs to be a faithful representation of the continues one, one has also to keep the compression of the DMRG in mind. We utilize the Julia language library ITensors [27] for the implementation of the DMRG algorithm and set the bond dimension compression error to 10^{-6}. This is sufficiently small such that the state derived from the DMRG is a valid representation of the uncompressed state, but large enough that the system is still computable on a normal PC.

To gauge the effects of the impurity one can look at the polaron energy which gives the energy it takes to immerse an impurity in the Bose gas:

$$E_P = E(g_{IB}) - E(0), \tag{A9}$$

where $E(0)$ is the ground-state energy of the system with $g_{IB} = 0$ and $E(g_{IB})$ is the corresponding ground-state energy

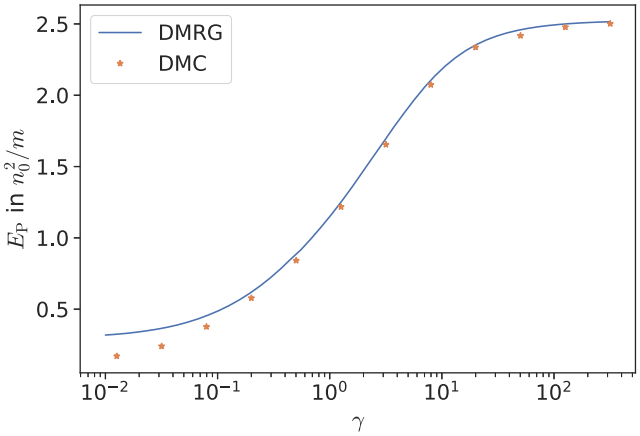

FIG. 13. Comparison of the saturated polaron energy ($g_{IB} = \infty$) for an immobile impurity ($M = \infty$) in a Bose gas with $N = 100$ particles from DMRG for OBC and diffusion quantum Monte Carlo results (DMC) for PBC from Ref. [9].

for a finite boson-impurity interaction. The polaron energy increases with g_{IB} but saturates for large interaction strength once the impurity has displaced all of the condensate at its position.

To benchmark our DMRG code we calculated the saturated polaron energy ($g_{IB} = \infty$) of an infinite-mass polaron ($M = \infty$) localized in the center of a 1D quasicondensate with $N = 100$ bosons for varying strength of the boson-boson interaction, quantified by γ and compared the results with those from diffusion quantum Monte Carlo (DMC) simulations taken from Ref. [9], see Fig. 13. The DMC simulations were done for periodic boundary conditions, while the DMRG data are for open boundary conditions, which explains the small difference for small value of γ. Open boundary conditions cause half dark solitons to form on each system edge for $\gamma \ll 1$ and Friedel oscillations for $\gamma \gg 1$ which increase the ground-state energy of the system compared with periodic boundary conditions. This was mostly negated here by choosing a system size which is large compared with the characteristic length scale of the system, the healing length $\xi = 1/\sqrt{2gn_0m}$ for $\gamma \ll 1$ or the wavelength of Friedel oscillations $2k_F = 2\pi n_0$ for $\gamma \gg 1$. Apart from very small γ values one recognizes excellent agreement. For small γ the polaron energies obtained with open boundary conditions (OBCs) as done in our DMR simulations are slightly larger than those obtained with periodic boundary conditions (PBCs) used in DMC as the spatial extent of the polaron, which is on the order of the healing length, becomes comparable to the system size:

$$\frac{L}{\xi} = \sqrt{2\gamma} N. \tag{A10}$$

Let us finally comment on some techniques to improve the numerical simulations. It turns out to be beneficial for the convergence of the DMRG algorithm to use a higher order representation of the second-order derivatives. So

$$\partial_x^2 \hat{\phi}(x) \approx \frac{-\frac{1}{12}\hat{a}_{i-2} + \frac{4}{3}\hat{a}_{i-1} - \frac{5}{2}\hat{a}_i + \frac{4}{3}\hat{a}_{i+1} - \frac{1}{12}\hat{a}_{i+2}}{\Delta x}. \tag{A11}$$

By inserting these transformations in the continuous Hamiltonian one arrives at

$$\begin{aligned}\hat{H} = &\sum_i \frac{1}{12}J(\hat{a}_i^\dagger \hat{a}_{i+2} + \text{H.c.}) - \frac{4}{3}J(\hat{a}_i^\dagger \hat{a}_{i+1} + \text{H.c.}) \\ &+ \frac{5}{2}J(\hat{a}_i^\dagger \hat{a}_i + \text{H.c.}) + U\hat{a}_i^\dagger \hat{a}_i^\dagger \hat{a}_i \hat{a}_i \\ &\times \frac{1}{12}J_I(\hat{b}_i^\dagger \hat{b}_{i+2} + \text{H.c.}) - \frac{4}{3}J_I(\hat{b}_i^\dagger \hat{b}_{i+1} + \text{H.c.}) \\ &+ \frac{5}{2}J_I(\hat{b}_i^\dagger \hat{b}_i + \text{H.c.}) + U_I\hat{b}_i^\dagger \hat{a}_i^\dagger \hat{a}_i \hat{b}_i. \end{aligned} \tag{A12}$$

As compared with a lattice Hamiltonian derived from (A3), the above expression (A12) contains longer-range hopping terms. These help the DMRG algorithm to establish correlations and therefore the algorithm is able to reach the ground state faster.

APPENDIX B: COMPARISON OF POLARON-POLARON INTERACTION POTENTIAL TO MEAN-FIELD RESULT

In the case of a weakly interacting Bose gas with $\gamma \ll 1$ the interaction potential between two Bose polarons in Born-Oppenheimer approximation can be determined semi-analytical [13]. One finds for repulsive interactions

$$\begin{aligned}V(r) = gn_0^2 r\left(\frac{1}{2} - \frac{4+2\nu}{3(\nu+1)^2}\right) + \frac{4}{3}\frac{gn_0^2\bar{\xi}}{\sqrt{1+\nu}}\Bigg\{&\sqrt{2\nu+2} \\ &+ 2\text{E}(\text{am}(u,\nu),\nu) \\ &- \frac{\sqrt{\nu}^3}{1+\nu}\text{cd}(u,\nu)^3[1+\sqrt{\nu}\,\text{sn}(u,\nu)] \\ &- \sqrt{\nu}\,\text{cd}(u,\nu)\left[\frac{3}{2} + \frac{1+2\nu}{1+\nu}\sqrt{\nu}\,\text{sn}(u,\nu)\right]\Bigg\}, \end{aligned} \tag{B1}$$

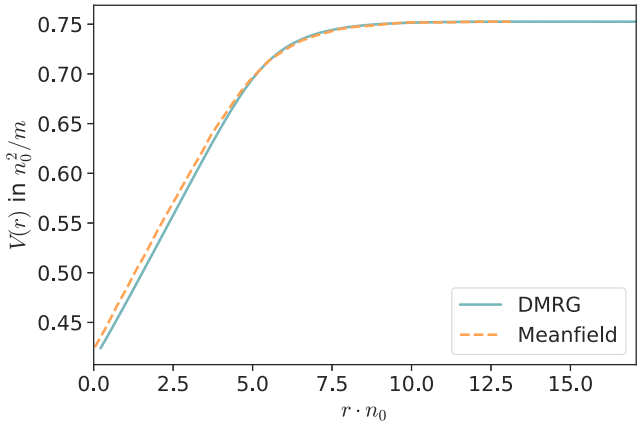

FIG. 14. Comparison of polaron-polaron interaction potential from mean-field calculations [13] (dashed lines) and from DMRG simulations (solid lines) for a boson-impurity interaction strength $g_{\text{IB}}\frac{m}{n_0} = 1.25$ and a weakly interacting Bose gas with $\gamma = 1/8$ and $N = 80$ particles.

where $u = r/(2\bar{\xi}\sqrt{1+\nu})$ is a normalized distance, $\text{E}(x,\nu)$ is the incomplete elliptic integral of the second kind, $\text{cd}(x,\nu)$ and $\text{sn}(x,\nu)$ are Jacobi elliptic functions and $\text{am}(x,\nu)$ is the amplitude of these functions [54]. The dimensionless parameter $\nu = \nu(r,\eta)$ with $|\nu| < 1$ is given implicitly by

$$2\frac{|\eta|}{n_0\bar{\xi}}\frac{\sqrt{\nu(\nu+1)}}{(1-\nu)}\ \text{cn}(u,\nu)\text{dn}(u,\nu) = [1+\sqrt{\nu}\text{sn}(u,\nu)]^2,$$

involving the Jacobi elliptic sn, cn, and dn functions and $\eta = g_{\text{IB}}/g > 0$. In general, this equation has several solutions, however, the physically relevant one is that with the largest ν.

In Fig. 14 we have shown a comparison of the DMRG results (full line) with the above prediction (dashed line).

[1] A. S. Alexandrov and J. T. Devreese, *Advances in Polaron Physics* (Springer-Verlag, Berlin, 2010), Vol. 159.

[2] M. A. Ruderman and C. Kittel, Indirect exchange coupling of nuclear magnetic moments by conduction electrons, Phys. Rev. **96**, 99 (1954).

[3] T. Kasuya, A theory of metallic ferro- and antiferromagnetism on Zener's model, Prog. Theor. Phys. **16**, 45 (1956).

[4] K. Yosida, Magnetic properties of Cu-Mn alloys, Phys. Rev. **106**, 893 (1957).

[5] L. N. Cooper, Bound electron pairs in a degenerate Fermi gas, Phys. Rev. **104**, 1189 (1956).

[6] D. Ter Haar, Electron motion in crystal lattices, *Collected Papers of L.D. Landau* (Pergamon, Bergama, 1965), Chap. 10, pp. 67–68.

[7] D. Ter Haar, The effective mass of the polaron, *Collected Papers of L.D. Landau* (Pergamon, Bergama, 1965), Chap. 67, pp. 478–483.

[8] H. Fröhlich, Electrons in lattice fields, Adv. Phys. **3**, 325 (1954).

[9] F. Grusdt, G. E. Astrakharchik, and E. Demler, Bose polarons in ultracold atoms in one dimension: beyond the Fröhlich paradigm, New J. Phys. **19**, 103035 (2017).

[10] T. D. Lee, F. E. Low, and D. Pines, The motion of slow electrons in a polar crystal, Phys. Rev. **90**, 297 (1953).

[11] A. G. Volosniev and H.-W. Hammer, Analytical approach to the Bose-polaron problem in one dimension, Phys. Rev. A **96**, 031601(R) (2017).

[12] J. Jager, R. Barnett, M. Will, and M. Fleischhauer, Strong-coupling Bose polarons in one dimension: Condensate deformation and modified Bogoliubov phonons, Phys. Rev. Res. **2**, 033142 (2020).

[13] M. Will, G. E. Astrakharchik, and M. Fleischhauer, Polaron interactions and bipolarons in one-dimensional Bose gases in the strong coupling regime, Phys. Rev. Lett. **127**, 103401 (2021).

[14] M. Will and M. Fleischhauer, Dynamics of polaron formation in 1D Bose gases in the strong-coupling regime, New J. Phys. **25**, 083043 (2023).

[15] G. Panochko and V. Pastukhov, Mean-field construction for spectrum of one-dimensional Bose polaron, Ann. Phys. (NY) **409**, 167933 (2019).

[16] E. Timmermans, Phase separation of Bose-Einstein condensates, Phys. Rev. Lett. **81**, 5718 (1998).

[17] D. K. K. Lee and J. M. F. Gunn, Polarons and Bose decondensation: A self-trapping approach, Phys. Rev. B **46**, 301 (1992).

[18] F. M. Cucchietti and E. Timmermans, Strong-coupling polarons in dilute gas Bose-Einstein condensates, Phys. Rev. Lett. **96**, 210401 (2006).

[19] K. Sacha and E. Timmermans, Self-localized impurities embedded in a one-dimensional Bose-Einstein condensate and their quantum fluctuations, Phys. Rev. A **73**, 063604 (2006).

[20] R. M. Kalas and D. Blume, Interaction-induced localization of an impurity in a trapped Bose-Einstein condensate, Phys. Rev. A **73**, 043608 (2006).

[21] M. Bruderer, W. Bao, and D. Jaksch, Self-trapping of impurities in Bose-Einstein condensates: Strong attractive and repulsive coupling, Europhys. Lett. **82**, 30004 (2008).

[22] A. A. Blinova, M. G. Boshier, and E. Timmermans, Two polaron flavors of the Bose-Einstein condensate impurity, Phys. Rev. A **88**, 053610 (2013).

[23] D. Brewer, U. of Sussex, I. U. of Pure, and A. Physics, *Quantum Fluids: Proceedings* (North-Holland Publishing Company, London, 1966).

[24] J. P. Hernandez, Electron self-trapping in liquids and dense gases, Rev. Mod. Phys. **63**, 675 (1991).

[25] L. Zschetzsche and R. E. Zillich, Suppression of polaron self-localization by correlations, Phys. Rev. Res. **6**, 023137 (2024).

[26] U. Schollwöck, The density-matrix renormalization group in the age of matrix product states, Ann. Phys. (NY) **326**, 96 (2011).

[27] M. Fishman, S. R. White, and E. M. Stoudenmire, The ITensor software library for tensor network calculations, SciPost Phys. Codebases 4 (2022).

[28] A. Recati, J.-N. Fuchs, C. S. Peca, and W. Zwerger, Casimir forces between defects in one-dimensional quantum liquids, Phys. Rev. A **72**, 023616 (2005).

[29] J. N. Fuchs, A. Recati, and W. Zwerger, Oscillating Casimir force between impurities in one-dimensional Fermi liquids, Phys. Rev. A **75**, 043615 (2007).

[30] N. D. Mermin and H. Wagner, Absence of ferromagnetism or antiferromagnetism in one- or two-dimensional isotropic Heisenberg models, Phys. Rev. Lett. **17**, 1133 (1966).

[31] P. C. Hohenberg, Existence of long-range order in one and two dimensions, Phys. Rev. **158**, 383 (1967).

[32] M. Girardeau, Relationship between systems of impenetrable bosons and fermions in one dimension, J. Math. Phys. **1**, 516 (1960).

[33] M. M. Nieto, Exact wave-function normalization constants for the $b_0 \tanh z - U_0 \cosh^{-2} z$ and Pöschl-Teller potentials, Phys. Rev. A **17**, 1273 (1978).

[34] A. Petković, B. Reichert, and Z. Ristivojevic, Density profile of a semi-infinite one-dimensional Bose gas and bound states of the impurity, Phys. Rev. Res. **2**, 043104 (2020).

[35] L. Parisi and S. Giorgini, Quantum Monte Carlo study of the Bose-polaron problem in a one-dimensional gas with contact interactions, Phys. Rev. A **95**, 023619 (2017).

[36] T. Cheon and T. Shigehara, Fermion-boson duality of one-dimensional quantum particles with generalized contact interactions, Phys. Rev. Lett. **82**, 2536 (1999).

[37] A. S. Alexandrov and A. B. Krebs, Polarons in high-temperature superconductors, Sov. Phys. Usp. **35**, 345 (1992).

[38] N. Mott, Polaron models of high-temperature superconductivity, Phys. C (Amsterdam, Netherlands) **205**, 191 (1993).

[39] A. S. Alexandrov and N. F. Mott, Bipolarons, Rep. Prog. Phys. **57**, 1197 (1994).

[40] J. L. Bredas and G. B. Street, Polarons, bipolarons, and solitons in conducting polymers, Acc. Chem. Res. **18**, 309 (1985).

[41] S. Glenis, M. Benz, E. LeGoff, J. L. Schindler, C. R. Kannewurf, and M. G. Kanatzidis, Polyfuran: a new synthetic approach and electronic properties, J. Am. Chem. Soc. **115**, 12519 (1993).

[42] M. N. Bussac and L. Zuppiroli, Bipolaron singlet and triplet states in disordered conducting polymers, Phys. Rev. B **47**, 5493 (1993).

[43] M. Fernandes, J. Garcia, M. Schultz, and F. Nart, Polaron and bipolaron transitions in doped poly(*p*-phenylene vinylene) films, Thin Solid Films **474**, 279 (2005).

[44] I. Zozoulenko, A. Singh, S. K. Singh, V. Gueskine, X. Crispin, and M. Berggren, Polarons, bipolarons, and absorption spectroscopy of PEDOT, ACS Appl. Polym. Mater. **1**, 83 (2019).

[45] P. A. Bobbert, T. D. Nguyen, F. W. A. van Oost, B. Koopmans, and M. Wohlgenannt, Bipolaron mechanism for organic magnetoresistance, Phys. Rev. Lett. **99**, 216801 (2007).

[46] M. Schecter, D. M. Gangardt, and A. Kamenev, Quantum impurities: From mobile Josephson junctions to depletons, New J. Phys. **18**, 065002 (2016).

[47] B. Reichert, A. Petković, and Z. Ristivojevic, Field-theoretical approach to the Casimir-like interaction in a one-dimensional Bose gas, Phys. Rev. B **99**, 205414 (2019).

[48] A. Petković and Z. Ristivojevic, Mediated interaction between polarons in a one-dimensional Bose gas, Phys. Rev. A **105**, L021303 (2022).

[49] M. Schecter and A. Kamenev, Phonon-mediated Casimir interaction between mobile impurities in one-dimensional quantum liquids, Phys. Rev. Lett. **112**, 155301 (2014).

[50] D. Huber, H.-W. Hammer, and A. Volosniev, In-medium bound states of two bosonic impurities in a one-dimensional Fermi gas, Phys. Rev. Res. **1**, 033177 (2019).

[51] A. G. Volosniev, H. W. Hammer, and N. T. Zinner, Real-time dynamics of an impurity in an ideal Bose gas in a trap, Phys. Rev. A **92**, 023623 (2015).

[52] A. S. Dehkharghani, A. Volosniev, and N. Zinner, Quantum impurity in a one-dimensional trapped Bose gas, Phys. Rev. A **92**, 031601(R) (2015).

[53] F. Gómez-Lozada, H. Hiyane, T. Busch, and T. Fogarty, Bose-Fermi N-polaron state emergence from correlation-mediated blocking of phase separation, arXiv:2409.13785.

[54] D. F. Lawden, *Elliptic Functions and Applications* (Springer, New York, NY, 1989).